



Contents lists available at ScienceDirect

Saudi Journal of Biological Sciences

journal homepage: www.sciencedirect.com

Application of high-fat cell model in steady-state regulation of vascular function

Qinghong Song^a, Yan Zhang^{b,*}

^a Department of Vascular Surgery, Tianjin People's Hospital (Nankai University Affiliated Hospital), Tianjin 300121, China

^b Department of Gynecology and Obstetrics, Tianjin 4th Center Hospital, Tianjin 300171, China



ARTICLE INFO

Article history:

Received 10 September 2019

Revised 21 September 2019

Accepted 24 September 2019

Available online 24 September 2019

Keywords:

High fat cell model

Endothelial cells

Vascular function

Disorder

ROS

ABSTRACT

In order to effectively apply the high-fat cell model to the regulation of vascular homeostasis and the repair of vascular endothelial cell injury, and to provide a new theoretical basis for the treatment of vascular homeostasis imbalance in the future, in this study, the mouse thoracic aorta tissue is extracted by using mouse endothelial cells. Western blotting and immunofluorescence resonance energy transfer (Immuno-FRET) are then used to verify the distribution and physical coupling properties of TRPV4 and Nox2 in cells. Finally, mouse mesenteric endothelial cells are isolated and cultured to induce FFA high-fat cell model. The results show that the nucleic acid expression levels of TRPV4 and Nox2 in RNA are significantly different from those of TRPV4 and Nox2 in protein. The relative values of TRPV4 and Nox2 in the control group are relatively low (0.8 ± 0.11). However, the relative values of TRPV4 and Nox2 are higher in the FFA high-fat cell model induced by the experimental group, and the values are (1.7 ± 0.8). Obviously, the relative values of TRPV4 and Nox2 in the experimental group are higher than those in the control group. The expression of reactive oxygen species (ROS) in vascular endothelial cells of control group is (1.0 ± 0.16), and that in FFA group is (2.5 ± 0.46). The expression of ROS in FFA cell model with HC067047A inhibitor is (1.5 ± 0.38). In the FFA cell model with apo inhibitor, ROS expression is (1.2 ± 0.23). Thus, in the FFA high-fat cell model induced successfully, the physical coupling of TRPV4 and Nox2 increases in primary endothelial cells, and the increase of physical coupling of TRPV4 and Nox2 results in the increase of ROS expression, which also means the imbalance of ROS homeostasis in vascular endothelial cells and the change of vascular endothelial cell permeability. The expression levels of TRPV4 and Nox2 are used as indicators of whether the vascular function is stable or unbalanced, thus providing a new theoretical basis for the treatment of cardiovascular diseases.

© 2019 Production and hosting by Elsevier B.V. on behalf of King Saud University. This is an open access article under the CC BY-NC-ND license (<http://creativecommons.org/licenses/by-nc-nd/4.0/>).

1. Introduction

In recent years, in the medical field, it has been found that reducing the bioavailability of NO and increasing the synthesis of vasoconstrictors and prostaglandins will directly lead to vascular dysfunction (Brignell et al., 2015). Moreover, vascular dysfunction can cause the imbalance of vascular endothelial cell homeostasis (Sarraf et al., 2015), resulting in cardiovascular diseases such as

diabetes, hyperlipidemia and hypertension (Webb et al., 2017), and ultimately lead to the formation of arterial thrombosis (Hammond et al., 2016). Vascular dysfunction is an imbalance between the bioavailability of nitric oxide and the accumulation of reactive oxygen species (ROS), which ultimately leads to endothelial dysfunction. Vascular endothelial injury can directly lead to vascular dysfunction. Vascular endothelial injury and dysfunction are also the main signs and important links of the occurrence and development of cardiovascular diseases such as obesity. Generally speaking, oxidative stress, oxidative cholesterol, cytokines, chemicals and low-density lipoproteins can cause damage to vascular endothelial cells (Kuo et al., 2014), thus causing imbalance of vascular homeostasis (González and Alonso-González, 2015). If the vascular homeostasis is unbalanced, it will lead to various diseases, such as obesity, hypertension, atherosclerosis, heart and kidney failure, coronary syndrome, thrombosis and diabetes. In

* Corresponding author.

E-mail address: zyan88@yahoo.com (Y. Zhang).

Peer review under responsibility of King Saud University.



obesity and other metabolic syndrome patients, plasma free fatty acids increase significantly (Sins et al., 2017) (see Figs. 1 and 2).

In the mouse model of high fat cells, the expression of ROS increases significantly. Increased ROS alter the biological function of mitochondria. Because of high fat, electrons in obese people are easily released from mitochondrial membrane complexes (Jenkins et al., 2016). The released electrons are easily combined with oxygen to produce a large amount of ROS, which can also lead to a large number of protons penetrating the mitochondrial cavity matrix, changing the mitochondrial membrane potential difference, thus promoting the apoptotic activation of mitochondrial signaling pathway, leading to vascular endothelial damage (Zhu et al., 2015). Obese patients lead to lower peroxide clearance, promote protein/lipid oxidation, promote the production of final glycosylation products, and significantly activate glycerol diester/protein kinase C signaling pathway, leading to vascular endothelial damage (Maneesai et al., 2016) (see Table 1).

Based on the above background, the high-fat cell model is effectively applied to the regulation of vascular homeostasis and repair of vascular endothelial cell injury. The mechanism of ROS produced by TRPV4 and Nox2 is studied, which can provide a new theoretical basis and experimental basis for the treatment of vascular endothelial injury and the maintenance of vascular homeostasis in the future.

2. Method

2.1. Research subjects

The rats used in the experiment are purchased through proper channels. After the rats are purchased, they are fed with standard rodent feed in the SPF level animal feeding barrier environment. The ambient humidity is maintained at 50%–55% and the ambient temperature is controlled at $21\text{ }^{\circ}\text{C} \pm 2\text{ }^{\circ}\text{C}$. Rats can drink water and eat freely, illuminated by light, and the illumination time is controlled at 12 h per day. It is necessary to add water and feed regularly, change the padding regularly, and weigh the rats regularly. The average weight of rats needs to be kept between 20 and 23 g.

2.2. Extraction of tissue mRNA

The mouse thoracic aorta tissue is isolated and fresh tissue the size of mung bean is put into a mortar. The mortar must be pre-cooled with liquid nitrogen before use. In a mortar, mouse thoracic aorta tissue is ground rapidly until it becomes powder. The ground powder structure is then placed in a pre-prepared RNAase FreeEP tube. 1 mL Trizol pyrolysis solution is added to EP tube. After

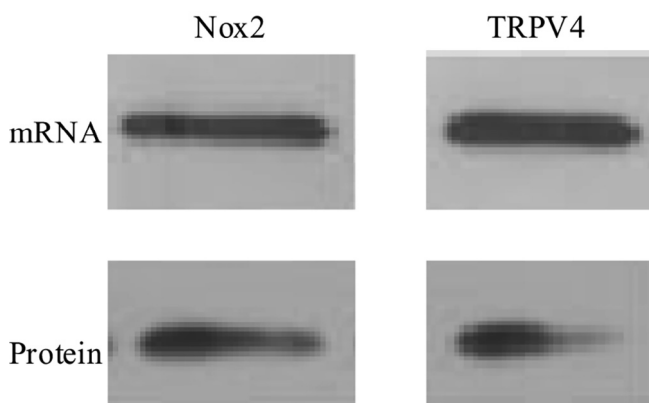


Fig. 1. Nucleic acid and protein expression levels of TRPV4 and Nox2.

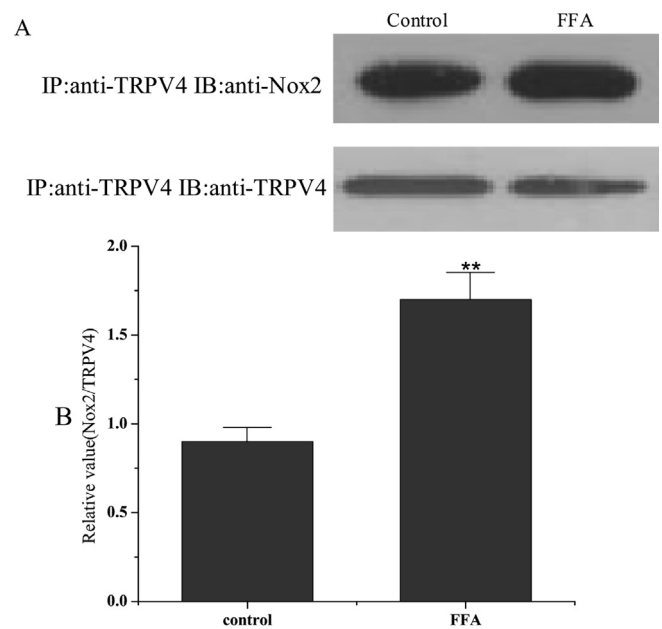


Fig. 2. Physical coupling of TRPV4 and Nox2 in normal endothelial cells and FFA cell models.

Table 1

Preparation of SDS-PAGE electrophoresis gel.

Separating gel components	13% Separating gel (10 mL)	Concentrated gel composition	5% concentrated gel composition (5 mL)
ddH ₂ O (mL)	3.5	ddH ₂ O (mL)	3.6
Tris-HCl (pH8.8) (mL)	2.3	Tris-HCl (pH8.8) (mL)	0.62
Arc-Bis (mL)	3.8	Arc-Bis (mL)	0.82
10%APS (ul)	110	10%APS (ul)	55
TEMED (ul)	6	TEMED (ul)	6

standing at room temperature for 3–5 min, RNAase Free's gunhead is used to blow the mixture, making it viscous and clear. The mixture is then moved to an EP tube with a capacity of 2 mL. 200 μL chloroform is added into EP tube, shaking and mixing, and it is kept at room temperature for 3–5 min. The centrifugal tube is centrifuged for 15 min at 12000rcf at $4\text{ }^{\circ}\text{C}$. The solution is divided into three layers, and the pipette is used to carefully suck out the upper water phase and add it to another centrifugal tube. 260 μL isopropanol is added to the initial amount of each mL TRIZOL, and the mixture is shaken and stirred. Then, it is placed at room temperature for 12–15 min. The supernatant is carefully removed after centrifugation for 10 min at $4\text{ }^{\circ}\text{C}$ with 12000rcf. 1 mL 75% ethanol is added to the precipitation and precipitate is washed. After centrifugation for 5 min at $4\text{ }^{\circ}\text{C}$ with 10000rcf, 75% ethanol is used to wash RNA precipitation again. The supernatant is removed and the specimens are dried in air for 8 min. When RNA is slightly transparent, the appropriate volume of RNase-free water is added and fully dissolved. Finally, RNA production is detected. The extracted RNA is preserved at $-80\text{ }^{\circ}\text{C} \pm 2\text{ }^{\circ}\text{C}$.

2.3. Extraction and determination of histone

The mouse thoracic aorta tissue is isolated and fresh tissue the size of mung bean is put into a mortar. The mortar must be pre-cooled with liquid nitrogen before use. In a mortar, mouse thoracic aorta tissue is ground rapidly until it becomes powder. The ground powder structure is then placed in a pre-prepared RNAase FreeEP

tube. Then, a mixture of 100 μ L protease inhibitor PMSF = 100:1 is added to the EP tube and pyrolyzed on ice for 0.5 h. Tissue fragments are liable to precipitate in the process of pyrolysis, so they can be fully cracked in mixed solution by oscillating and mixing with a pipette gun from time to time. After 0.5 h, the specimens are centrifuged at 4 °C 10000g for 20 min, and the supernatant is transferred to a pre-cooled plastic tube. BCA method is used to detect protein concentration. The concentration of BCA is diluted to 0.6 mg/mL, and BCA is added to 96-well plate in turn. Then, 220 μ L BCA working fluid is added to the standard. Subsequently, 220 μ L BCA working fluid is also added to the sample to be tested. The incubation time is 0.5 h at 37 °C \pm 2 °C. Finally, the enzyme labeling instrument is used to determine the absorbance of protein and draw the curve. According to the graph, the concentration of histone is calculated.

2.4. Isolation and culture of mouse arterial endothelial cells

When the central nervous system lost control of the whole body and the animal is unconscious, the rats are killed by cervical dislocation, and the mesentery of the rats is immediately separated and removed. Then, the removed mesentery is quickly put into PBS buffer. The mesenteric tegmentum of rats is cut with surgical scissors at a growth rate of about 2.5 cm. These segments of the mouse mesentery are then transferred to the flask of the EBM basic medium. The mesentery of rats is slowly digested for 50 min in a shaking water bath at 37 °C. 1.5 mL ECM complete medium is added to a shaking water bath to terminate mesenteric digestion.

The liquid is transferred to an EP tube with a pre-prepared capacity of 10 mL. After centrifuging for 5 min in a 1000 rpm cryogenic centrifuge, the supernatant is carefully and slowly removed, leaving sediment at the bottom. The ECM complete medium of 1.5 mL is added into the precipitate of EP tube, and is mixed by oscillation. The suspension is transferred to a clean culture bottle, and the ECM complete culture medium is added until the volume of the mixed solution is 3 mL. Finally, the mixed solution in the culture bottle is put into the cell culture box. In order to carry out the follow-up experiment normally, after 2 h, PBS buffer is used to wash mesenteric endothelial cells after mesenteric endothelial cells adhere to the wall, and then ECM complete medium is added until the volume of the mixed solution is 3 mL.

2.5. Induction of high fat cell model

Firstly, NaOH with a mass of 0.03 g is added to 12 mL ddH₂O to make it fully dissolved. After filtration, NaOH solution with concentration of 0.1 mol/L is obtained. Bovine serum albumin (BSA) with mass of 1 g is added to the buffer of PBS to dissolve it sufficiently. Then, it is filtered after 6 min in a water bath at 37 °C to obtain 10% BSA solution. A certain amount of palmitic acid is added to the 0.1 mol/L NaOH solution to make it fully react and dissolve. Palmitic acid storage solution with solubility of 4 mM is obtained by water bath at 65 °C \pm 2 °C for 0.5 h. Similarly, a certain amount of oleic acid is added to the 0.1 mol/L NaOH solution prepared above to make it fully react and dissolve. Oleic acid storage solution with a concentration of 2 mM can be obtained by water bath for 0.5 h at 65 °C \pm 2 °C. 10% BSA solution is taken and 1.5 mL palmitic acid storage solution is added to the solution. Next, 1.5 mL oleic acid storage solution is added. It is fully dissolved in water bath for 0.5 h at 37 °C, and then filtered. The above steps describe the preparation of FFA medium.

2 mL NaOH solution of 0.1 mol/L is mixed with 10 mL 10% BSA solution to dissolve them fully. It is fully dissolved in water bath for 0.5 h at 37 °C, and then filtered. The above solution is added to the ECM complete medium. The concentration of BSA solution is kept

at 0.8%, while that of NaOH solution is kept at 0.2%, and then filtered. At this time, the control medium is prepared.

Finally, high-fat cells need to be induced. After treatment, the primary endothelial cells are laid on the surface of the six-well plate, and the solubility of the endothelial cells reaches about 50%. Then, it is cultured in a Petri dish for 12 h. After the mesenteric endothelial cells are fully adhered, the control medium and FFA high-fat medium are replaced. After culturing the induced cells for 1 day, they can be successfully induced into FFA high-fat cell model.

2.6. Statistical analysis method

The measurement data are expressed by mean \pm standard deviation ($\bar{x} \pm s$). The measurement data are tested by normality test, and the data are processed by SPSS18.0 software. Chi-square test is used to compare the mean of multiple samples, and *t*-test is used between two independent samples. *P* < 0.05 shows significant difference, and the difference is statistically significant.

3. Results and discussion

3.1. Expression of TRPV4 and Nox2 in normal rats

The thoracic aorta of rats is separated and ground. Tissue mRNA is extracted after grinding. Reverse transcription-polymerase chain reaction (RT-PCR) is used to monitor the nucleic acid expression of TRPV4 and Nox2 in vascular tissues of rats. Meanwhile, the thoracic aorta of rats is separated and ground. After grinding, tissue proteins are extracted. Western blotting method is used to detect the expression of TRPV4 and Nox2 proteins in vascular tissues of rats. As shown in the figure below, there is a significant difference between the nucleic acid expression levels of TRPV4 and Nox2 in mRNA and the protein expression levels of TRPV4 and Nox2 in protein.

3.2. Physical coupling of TRPV4 and Nox2 in endothelial cells under FFA

As shown in the figure below, the results are counted through GraphPad Prism5.0. The relative values of TRPV4 and Nox2 in the control group are relatively low (0.8 ± 0.11). However, the relative values of TRPV4 and Nox2 are higher in the FFA hyperlipidemia cell model induced by the experimental group, and the values are (1.7 ± 0.8). Obviously, the relative values of TRPV4 and Nox2 in the experimental group are higher than those in the control group. Statistical analysis shows that there is statistical significance (*P* < 0.01). Thus, there is a physical coupling relationship between TRPV4 and Nox2 in primary endothelial cells, and the physical coupling of TRPV4 and Nox2 in primary endothelial cells increases in the FFA hyperlipidemia cell model induced successfully.

3.3. ROS expression in FFA cell model

DCFH-DA Reactive Oxygen Kit is used to label ROS produced in mouse vascular endothelial cells. The results are shown in Fig. 3A. From Fig. 3B, it can be seen that the ROS expression in vascular endothelial cells of the control group is (1.0 ± 0.16), the ROS expression in the endothelial cells of the FFA group is (2.5 ± 0.46), the ROS expression in the FFA cell model with HC067047A inhibitor is (1.5 ± 0.38), and the ROS expression in the FFA cell model with Apo inhibitor is (1.2 ± 0.23). Thus, compared with the control group, the expression of ROS in the FFA cell model of the experimental group is 2.5 times higher than that of the control group. Moreover, the addition of HC067047A inhibitor and Apo inhibitor can effectively control the production of ROS in

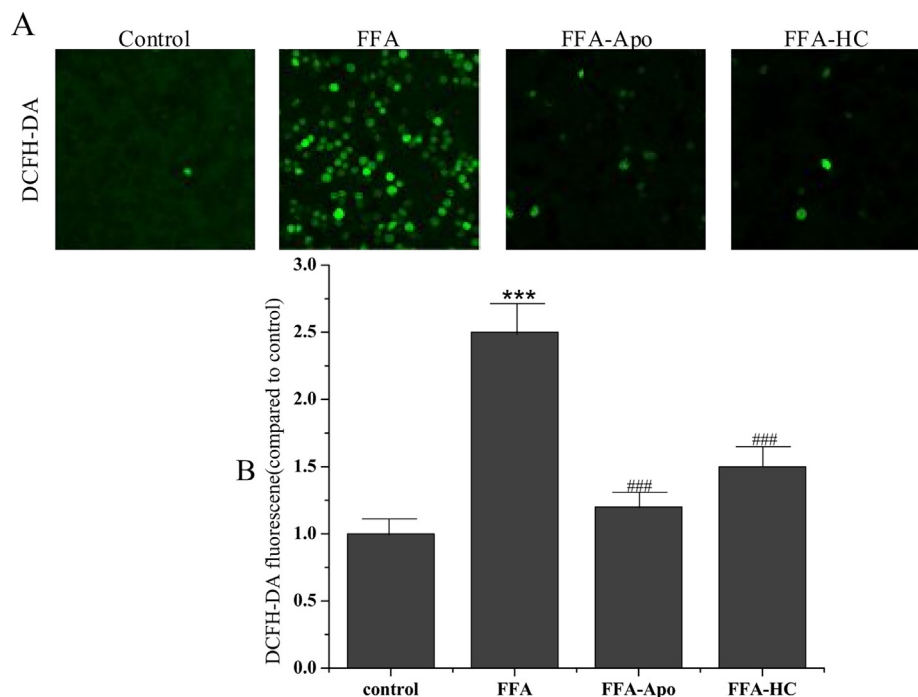


Fig. 3. Detection of ROS production in normal endothelial cells and FFA cell models with DCFH-DA.

FFA cell model. Compared with the control group, the FFA model group has significant difference, with statistical significance ($P < 0.01$). The difference between FFA-Apo group and FFA-HC group and FFA cell model group is statistically significant ($P < 0.05$).

4. Discussion

In this experiment, first of all, RT-PCR and Western blotting analysis are used to demonstrate the presence of TRPV4 and Nox2 in mouse endothelial cells. Then, immunofluorescence resonance energy transfer experiment is used to directly prove the physical coupling between TRPV4 and Nox2. Finally, the successfully induced FFA cell model is utilized. Compared with the control group, the expression of ROS in the FFA cell model of the experimental group is 2.5 times higher than that of the control group. Moreover, the addition of HC067047A inhibitor and Apo inhibitor can effectively control the production of ROS in FFA cell model. The increase of physical coupling between TRPV4 and Nox2 in primary endothelial cells of FFA cell model leads to the increase of ROS expression, which means the imbalance of ROS homeostasis and the change of permeability of vascular endothelial cells. This further explains the causes of endothelial cell dysfunction.

Although some experimental results have been obtained, there are still many shortcomings. Firstly, only the roles of TRPV4 and Nox2 proteins in the regulation of vascular homeostasis are studied in this study. However, when endothelial vascular dysfunction or imbalance occurs, there is not only these two proteins change. In addition, due to time constraints, the specific mechanisms of TRPV4 and Nox2 and the changes of related signaling pathways have not been studied. Moreover, the original plan is to knock

out the Nox2 gene in rats, but in the end, no related experiments are carried out.

References

- Brignell, J.L., Perry, M.D., Nelson, C.P., 2015. Steady-state modulation of voltage-gated K⁺ channels in rat arterial smooth muscle by cyclic AMP-dependent protein kinase and protein phosphatase 2B. *PLoS ONE* 10 (3), e0121285.
- González, M.C., Alonso-González, 2015. Melatonin affects the dynamic steady-state equilibrium of estrogen sulfates in human umbilical vein endothelial cells by regulating the balance between estrogen sulfatase and sulfotransferase. *Int. J. Mol. Med.* 36 (6), 1671–1676.
- Hammond, Kelly M., Impey, Samuel G., Currell, K., 2016. Postexercise high-fat feeding suppresses p70S6K1 activity in human skeletal muscle. *Med. Sci. Sports Exercise* 48 (11), 2108.
- Jenkins, T.A., Nguyen, Jason C.D., Hart, J.L., 2016. Decreased vascular H2S production is associated with vascular oxidative stress in rats fed a high-fat western diet. *Naunyn-Schmiedeberg's Arch. Pharmacol.* 389 (7), 783–790.
- Kuo, Y., Abdullaev, I.F., Hyzinski, G., María, C., 2014. Effects of alternative splicing on the function of bestrophin-1 calcium-activated chloride channels. *Biochem. J* 458 (3), 575–583.
- Maneesai, P., Bunbupha, S., Kukongviriyapan, U., 2016. Asiatic acid attenuates renin-angiotensin system activation and improves vascular function in high-carbohydrate, high-fat diet fed rats. *Bmc Complementary Altern. Med.* 16 (1), 1–11.
- Sarraf, M., Perles-Barbacaru, Teodora, Adriana, Nissou, Marie France, 2015. Rapid-Steady-State-T₁ρ signal modeling during contrast agent extravasation: Toward tumor blood volume quantification without requiring the arterial input function. *Magn. Reson. Med.* 73 (3), 1005–1014.
- Sins, Joep W.R., Schimmel, Marein, Luken, Brenda M., 2017. Dynamics of von Willebrand factor reactivity in sickle cell disease during vaso-occlusive crisis and steady state. *J. Thromb. Haemostasis* 15 (7), 1392–1402.
- Webb, G.F., Villella-Bressan, R., Dyson, J., 2017. The steady state of a maturity structured tumor cord cell population. *Discrete Continuous Dynamical Syst. – Ser. B (DCDS-B)* 4 (1), 115–134.
- Zhu, Y., Paul, P., Lee, S., 2015. Antioxidant inhibition of steady-state reactive oxygen species and cell growth in neuroblastoma. *Surgery* 158 (3), 827–836.